Remotely sensed localised primary production anomalies predict the burden and community structure of infection in long-term rodent datasets

Running title: **Habitat greening predicts infection burden**

Joseph A. Jackson[1], Anna Bajer[2], Jolanta Behnke-Borowczyk[3], Francis S. Gilbert[4], Maciej Grzybek[5], Mohammed Alsarraf[2] and Jerzy M. Behnke[4]

ORCID IDs:

JAJ: 0000-0003-0330-5478

AB: 0000-0001-6199-8458

JBB: 0000-0003-2085-038X

FSG: 0000-0002-2727-4103

MG: 0000-0002-8780-0304

MA: 0000-0002-6330-0719

JMB: 0000-0001-9396-2572

1. School of Science, Engineering and Environment, University of Salford, Manchester M5 4WT, UK

2.Department of Eco-Epidemiology of Parasitic Diseases, Institute of Developmental Biology and Biomedical Sciences, Faculty of Biology, University of Warsaw, Miecznikowa 1, 02-096 Warsaw, Poland

3. Department of Forest Pathology, Faculty of Forestry, Poznań University of Life Sciences, 71C Wojska Polskiego Street, 60-625 Poznań, Poland

4. School of Life Sciences, University of Nottingham, University Park, Nottingham NG7 2RD, UK

5. Department of Tropical Parasitology, Institute of Maritime and Tropical Medicine, Medical University of Gdansk, 81-519 Gdynia, Poland

Contact information:

Professor J.A. Jackson; E-mail J.A.Jackson@Salford.ac.uk; Tel +44 7432 219376

Professor J.M. Behnke; E-mail Jerzy.Behnke@Nottingham.ac.uk

Abstract

The increasing frequency and cost of zoonotic disease emergence due to global change has led to calls for the primary surveillance of wildlife. This should be facilitated by the ready availability of remotely-sensed environmental data, given the importance of the environment in determining infectious disease dynamics. However, there has been little evaluation of the temporal predictiveness of remotely-sensed environmental data for infection reservoirs in vertebrate hosts due to a deficit of corresponding high-quality long-term infection datasets. Here we employ two unique decade-spanning datasets for assemblages of infectious agents, including zoonotic agents, in rodents in stable habitats. Such stable habitats are important, as they provide the baseline sets of pathogens for the interactions within degrading habitats that have been identified as hotspots for zoonotic emergence. We focus on the Enhanced Vegetation Index (EVI), a measure of vegetation greening that equates to primary productivity, reasoning that this would modulate infectious agent populations via trophic cascades determining host population density or immunocompetence. We found that EVI, in analyses with data standardised by site, inversely predicted more than one third of the variation in an index of infectious agent total abundance. Moreover, in bipartite host occupancy networks, weighted network statistics (connectance and modularity) were linked to total abundance and were also predicted by EVI. Infectious agent abundance and, perhaps, community structure are likely to influence infection risk and, in turn, the probability of transboundary emergence. Thus, the present results, which were consistent in disparate forest and desert systems, provide proof-of-principle that within-site fluctuations in satellite-derived greenness indices can furnish useful forecasting that could focus primary surveillance. In relation to the well documented global greening trend of recent decades, the present results predict declining infection burden in wild vertebrates in stable habitats; but if greening trends were to be reversed, this might magnify the already upwards trend in zoonotic emergence.

KEYWORDS

EVI, greening, parasites, infectious agents, community networks, connectance, modularity, wild rodent, zoonotic reservoir, time series

1 | INTRODUCTION

Given the human and economic cost of infectious disease emergences from wildlife reservoirs (Häsler et al., 2013; Dobson et al., 2020; Bernstein et al., 2022), the primary surveillance of infection risks from wildlife seems increasingly warranted. For this purpose, environmental variation should be a particularly valuable source of predictive information. This is due to the importance of the environment in driving infection dynamics and to the ready availability of fine-grained, near-real-time, satellite-derived environmental measurements on a global scale. Despite this potential, our ability to use satellite (remotely-sensed) data to forecast temporal fluctuations in the pattern of infection in wild vertebrates is currently limited. In particular, the evaluation of candidate predictors is restricted by a lack of corresponding high-quality infection data time series (Wille et al., 2021; Becker at al., 2023). Here we employ two decade-spanning rodent infection datasets whose regular multiannual sampling regimens make them uniquely suitable to assess whether remotely-sensed environmental measurements have forecasting power for the abundance and structure of natural infectious agent communities. Crucially, such variation in the burden of infection (Plowright et al., 2017), and in infectious agent community structure (Bordes & Morand, 2009), might be expected to relate to infectious disease risk in wildlife, and thence to the risk of zoonotic or transboundary emergence from wildlife reservoirs. The infection data time series we employ (described further below) are for broad multispecies infectious agent assemblages in two different hosts occupying different biomes and have previously been extensively documented (Behnke et al., 2000, 2001, 2004, 2008a, b, 2019; Grzybek et al., 2015; Alsarraf et al., 2016). For prediction, we specifically focus on the remotely-sensed Enhanced Vegetation Index (EVI) (Huete et al., 2002), a measure of “greenness” reflecting primary production in plants (Sims et al., 2006). EVI is related to the widely used Normalized Difference Vegetation Index (NDVI) but corrects for atmospheric conditions and canopy background variations (Huete et al., 2002). Importantly, we expected primary production to be especially informative as it is likely to have an ultimate local causal influence upon key proximal drivers of infection (Parmenter et al., 1999; Glass et al., 2002; Xu et al., 2015; King'ori, 2020; Eby et al., 2023). These proximal drivers could include host density (Santini et al., 2018) and host immunocompetence (Jackson et al., 2020), which are likely to be influenced by bottom-up trophic cascades (Parmenter et al., 1999) dependent on primary production. The causal influence of primary production might manifest itself, for example (and non-exhaustively), through the augmentation of food availability, increasing host abundance and altering infection dynamics as a result. A similar process has been suggested to explain links between the El Niño Southern Oscillation and hantavirus outbreaks in the southwestern United States (Glass et al., 2002). Alternatively, diminished

primary production might result in food shortage, interference with host immune function and promotion of infectious disease transmission (Jackson et al., 2020).

Due to a deficit of high-quality long-term time series with regular sampling design, most efforts at predicting the burden of infection in natural systems through the remote-sensing of vegetation state (or through otherwise measured correlates of vegetation state), are focussed on spatial variation (between sites) or within-year data. This has limitations for forecasting (i.e., predicting into the future) locally, which may be an important goal for surveillance. For example, in the case of spatial studies, the determinants of spatial variation, although they might be extrapolated to predict longer term temporal scenarios under land usage or climate change, may not be the same as the determinants of temporal variation on other scales. In particular, spatial designs may be uninformative for local temporal forecasting because drivers of temporal variation (perhaps including primary productivity) may be unrelated to important site-specific determinants of infectious assemblages. The latter could, for instance, include the nature of the substrate, or the animal species present (Carlson et al., 2022; Stenseth et al., 2022). Moreover, in the case of within-year data, autocorrelation is problematical, as any regular seasonal variables will correlate at certain times of the year, given a certain time lag. In contrast, in the present study, we focus particularly on long-term within-site between-year temporal variation, with sampling points at the same time of year. For this, we reasoned that if primary production (represented by remotely-sensed vegetation measures) is a driver of temporal infection dynamics, then this will have a more detectable signal on a level playing field within sites and at the same phase point in the circannual cycle.

Previous studies on the environmental drivers of infection burden in nature have also often only considered individual or limited groups of pathogen species, but a focus on wider species communities, as we adopt here, may provide more information. Thus, for analyses of abundance, an overall measure of abundance, grouped across the infectious agent community (e.g., via latent variables from multivariate analyses, or overall means of standardised abundance, as we use here) has advantages. Such a measure would tend to reflect overarching drivers (and not species-specific drivers) and also tends, in practice, to produce a well-conditioned variable for statistical analysis (with a less skewed distribution), increasing sensitivity. Moreover, enumerating established individuals across complex communities, as we have carried out here, allows the analysis of the structure of those communities. This is relevant to our current focus on forecasting infection risk, because host permissiveness to transmission may be determined by the manner of infectious agent community assembly due to the regulatory properties of interspecific interactions (Gotelli et al., 2017; de Vos et al., 2017). Below we calculated structural metrics for bipartite networks

(Dormann et al., 2008; Poulin, 2010) of host occupancy as these may affect the stability and regulation of communities (May, 1972; Grilli et al., 2016; Delmas et al., 2019).

Rodents, alongside bats, are the greatest reservoir for zoonotic infectious agents (Luis et al., 2013; Han et al., 2016). In the present study, the rodent infection time series data that we employ include zoonotic agents such as *Babesia* (see Young et al., 2019) and *Bartonella* (see Krügel et al., 2022), although we would expect any community-wide responses observed to be the most interesting from a general point of view. The present time series span the 2001-2010 decade with multiple time points. This decade was claimed to be the warmest and fastest-warming decade in historical records until 2010, and to encompass major climate perturbation (WMO, 2013). The time series also represent very divergent rodent host-infectious agent systems in disparate biomes and so consistent trends in both would point towards the existence of general, widely relevant, processes. Thus, one of the time series is for bank voles (*Myodes glareolus*) in the temperate zone, forested ecosystems of the Mazury Lake District in North-Eastern Poland. The other is for spiny mice (*Acomys dimidiatus*) in the subtropical desert, wadi ecosystems of the St Katherine Protectorate, South Sinai, Egypt. In both cases, the infection data consist of direct visual counts of infectious agents based on invasive sampling at autopsy and are likely to be more precise than indirect measurements featuring in many studies, such as serology, PCR diagnostics or propagule counts in faeces. Uniquely, each of these contrasting time series has a regular, standardised sampling design that includes quantification of metazoan parasites, haemoparasites and haemopathogens and host biometric data. Each also has site replication of distinctive localities, sampled consistently through time points. Thus in practice, when data grouping is taken into account, this has allowed sufficient degrees of freedom to detect overall association between site-level time-point observations for infectious agent community metrics and vegetation indices derived from remote sensing measurements.

In summary, in this study, using the datasets described above, we calculate an index of overall infectious agent abundance, as this would be expected to be linked to infection risk. (Here and below, we take infection risk to mean risk within the studied populations but also, ultimately, transboundary risk.) We additionally derive network statistics for bipartite networks of host occupancy as these might contribute to infection risk through effects on community regulation and stability. Accounting for confounding variation, and standardising data within sites prior to analysis (i.e., converting the data to within-site anomalies), we ask whether any of these quantities are predicted by inter-annual EVI fluctuations within sites. Our findings suggest that site-standardised EVI is indeed substantially predictive of infectious agent abundance and network structure. We argue that this highlights the need for future work to understand the causal mechanisms involved and to further establish the

practical potential for forecasting infection risk using EVI. We also point out that the associations we observed would predict a suppression of infection risk in stable habitats in recent decades, given worldwide greening trends (Zhu et al., 2016), but we note that this could be reversed in the case that greening trends are not maintained (Winkler et al., 2021).

2 | MATERIALS AND METHODS

2.1 | Overview

In this study we set out to assess the degree to which infectious agent abundance and community structure can be predicted by remotely-sensed vegetation greenness. We employed long-term datasets for two contrasting rodent - infectious agent systems with regular, site-replicated sampling designs and individual count data for a wide range of infectious agents. For these datasets, we calculated overall indices of infectious agent abundance and network statistics for host occupancy networks. To represent greenness, we used the publicly-available Enhanced Vegetation Index (EVI) data product. Importantly, we reasoned that, within each host-infectious agent system, individual sites would be subject to many idiosyncratic site-specific constraints on infectious agent abundance and community structure, on the one hand, and on EVI, on the other, that might lead these to vary independently (obscuring any functional link). Such constraints might include, for example, faunal composition, habitat connectivity or substrate characteristics, in the case of infectious agents, or floral composition, soil composition or canopy structure in the case of EVI. On the other hand, within-site changes in vegetation greenness and infectious agents over time, upon a relatively level playing field for site-specific constraints, would be more likely to reveal a functional relationship between the two. Thus, crucially, in the analyses below, we standardised (zero mean, unit standard deviation) the infection variables and EVI within sites prior to linear statistical modelling.

2.2 | The study systems

Infection data for this study are based on multi-year, late summer, sampling of bank voles (*Myodes glareolus*; Cricetidae) at 3 defined sites in the Mazury Lake District in North-Eastern Poland and of spiny mice (*Acomys dimidiatus*; Muridae) at 4 defined sites in St. Katherine's Protectorate, Sinai, Egypt. The Polish sites, Urwitałt (53.80255, 21.663067), Talłty (53.894067, 21.550817) and Pilchy (53.7038, 21.808317) (Behnke et al., 2001; Grzybek et al., 2015), in the Central European mixed forest ecoregion (Olson et al., 2001), were situated along an approximately northeast to southeast 27 km transect and were separated by physical barriers and habitat unsuitable for bank voles. The sites were mainly forested

(Behnke et al., 2001), featuring a mature canopy dominated by *Pinus sylvestris* and *Betula verucosa*, but also containing *Picea abies*, *Quercus robur* and *Alnus glutinosa*; shrub layers consisted mainly of *Corylus avellana* and ground cover was primarily by *Oxalis acetulosa*, *Convalaria mayalis*, *Stelaria holostea* or moss. Small gladed areas occurred within the forests, dominated by grasses. The Egyptian sites, in the Arabian desert ecoregion (Olson et al., 2001), were discrete montane wadi habitats at El Arbein (28.553440, 33.94796), Gebal (28.53342, 33.908398), Gharaba (28.64672, 33.88991) and Tlah (28.56452, 33.93682) situated within 12 km of St Katherine, South Sinai. The wadis are hyper-arid environments with sparse rainfall in December-February only. Natural vegetation cover is <10%, but the wadi floors are partly covered by oasis-like walled orchard gardens that employ rainwater harvesting to maintain a year-round presence of crop plants amongst which wild desert annual and perennial vegetation also grows (Norfolk et al., 2012, 2013, 2015).

2.3 | Sampling

The three Polish sites were sampled in 1999, 2002, 2006 and 2010 and the four Egyptian sites were sampled in 2000, 2004, 2008 and 2012. The 1999 data fell before the availability of the remotely-sensed data product used here (see below) and were thus not included directly in the main analyses of data aggregated by site, although they were included in supporting analyses of unaggregated individual host data. Sampling methods, and the respective compositions of the infectious agent communities, have been previously described for both the Polish bank vole and Egyptian spiny mice systems. In brief, for both systems, hosts were captured by humane live-trapping in a 3-4 week trapping campaign starting in mid-August and killed and autopsied shortly after capture. For the Egyptian sites, sampling was based on a total of 52076 trap hours (1838-5244 per site × year combination) and for the Polish sites (for 2002-2010) 172271 trap hours (9356-34363 per site × year combination). For the Egyptian spiny mice, the traps were placed along wadi floors, primarily in and around walled gardens (Behnke et al., 2000). Biometric data (sex and weight) were recorded for hosts and, in the case of *M. glareolus* samples, order-level counts were made of ectoparasitic fleas (Siphonaptera) and ticks (Ixodida). For all samples, metazoan endoparasites occurring in the gastrointestinal tract or the body cavity were identified to species level and enumerated. In a very small minority of cases unidentified endoparasite specimens were placed in phylum-level categories. Haemoparasites (*Babesia*, *Hepatozoon* and *Trypanosoma*) and haemopathogens (*Bartonella* and *Mycoplasma*), identified to genus level, were quantified by microscopic counts of stages on peripheral blood smears. The Polish data set contained 21 taxon groupings (2 arthropod, 3 protozoan, 2 bacterial, 8 nematode and 6 cestode) and the Egyptian dataset 26 taxon groupings (3 protozoan, 2 bacterial, 13 nematode, 7 cestode and 1 acanthocephalan).

For analysis of the Polish dataset, hosts with any missing infection or biometric data were excluded. Final sample size was 812 voles for the full Polish dataset (35-97 per year × site combination, mean = 68) and 689 voles (56-97 per year × site combination, mean = 77) when 1999 data were excluded. For analysis of abundance in the Egyptian dataset, hosts with any missing data were excluded, giving a final sample size of 419 (6-42 per year × site combination, mean = 26). For network analysis of the Egyptian dataset, only hosts with missing infectious agent data were excluded (as there were proportionately more missing biometric data in this dataset and these data were not used in the networks); sample size was 427 (11-42 per year × site combination, mean = 27).

2.4 | Enhanced vegetation index (EVI) data

Enhanced Vegetation Index (EVI) (Huete et al., 2002) data (MOD13Q1 data product (Didan & Huete, 2015)) corresponding to spatial polygons for the study sites (see Supplementary Table 1) were downloaded via the National Aeronautics and Space Administration (NASA) AppEEARS application (AppEEARS Team, 2023). MOD13Q1 data is derived from the Terra Moderate Resolution Imaging Spectroradiometer instrument for 16-day intervals at 250m resolution and is based on atmospherically-corrected reflectance in the red, near-infrared and blue wavebands. EVI differs from the older, related NDVI (Normalized Difference Vegetation Index) metric by attempting to correct for atmospheric and background effects and may be superior in discriminating areas of high-density vegetation where NDVI saturates (Didan et al., 2015). The average EVI for 3 months of data prior to the month of sampling was employed for all analyses (see Supplementary Table 2), as similar timeframes have been used in studies relating NDVI, or its correlates, to infectious agent populations (King'ori et al., 2020; Shearer & Ezenwa, 2020; Rubenina et al., 2021). EVI is widely accepted to capture vegetation phenology and primary productivity variation in forest and grassland biotypes (Huete et al., 2002; Sims et al., 2006; Huete, 2012; Zhou et al., 2014; Fernández et al., 2016; Shi et al., 2017), such as the Polish sites here, which were mainly gladed forests. EVI or NDVI have also been employed to monitor vegetation in hyper-arid environments (Saltz et al., 1999; Wallace & Thomas, 2008; Wang et al., 2014; Chávez et al., 2019; Moat et al., 2021), such as the Egyptian sites here, and also at other desert localities in the Sinai peninsula (Dall'Olmo & Karnieli, 2002). EVI variables for the present Egyptian sites had a clear seasonal fluctuation with, as might be expected if vegetation is represented, a nadir at the start of the rainy season.

2.5 | An overall measure of infectious agent abundance

To calculate an overall index of infection abundance (Total abundance Index, TAI) for hosts within each of the two sample sets (Egypt and Poland) we first standardised the counts for

each infectious agent taxon for all hosts in the sample set (zero mean, unit standard deviation) and then summed the standardised counts for each host:

$$TAI' = \sum_{j=1}^{p} \sum_{i=1}^{n} \frac{X-\mu}{\delta},$$

where n = the number of hosts in the sample set, p = the number of infectious agent species in the sample set, X = abundance of the j^{th} infectious agent species in the i^{th} host, μ = mean abundance for the j^{th} infectious agent species in the host population and δ = the standard deviation for abundance of the j^{th} infectious agent species in the host population.

Within each sample set the distribution of the resulting index was less skewed than the individual infectious agent variables but still non-normal, so the index variable was rescaled 1-101 and a log transformation was applied (where *max* is the maximum value for *TAI'*, and *min* is the minimum value):

$$TAI = log_{10}\left(\left(\left(\frac{TAI'-min}{max-min}\right)100\right)+1\right).$$

2.6 | Network statistics

Network analyses were carried out in *R* version 4.2.1 (R Core Team, 2022). The *bipartite* package (Dormann et al., 2008) was employed to construct a separate weighted bipartite network for each site × year dataset, joining individual hosts and infectious agent taxa, where edge weights corresponded to the $\log_2 (x + 1)$ transformed raw infectious agent counts. Weighted network statistics (modularity, connectance and nestedness) were calculated for each network (Dormann et al., 2009). Modularity, connectance and nestedness were selected as they have been linked with community stability or regulation in the literature (Delmas et al., 2019; Poulin & McDougall, 2022). Weighted modularity (Q) reflects the weight of edges inside modules compared to outside modules, where a module is defined as an edge rich cluster within a community (Dormann & Strauss, 2014). Weighted connectance reflects the weights of realised relative to possible edges in a network (Bersier et al., 2002). Weighted nestedness is the tendency for edges of a given node to form a subset of the edges of nodes of higher degree (i.e., nodes with more edges), taking the weight of edges into account. The weighted nestedness measure used here increases with nestedness and was calculated following the WNODF (Weighted Nestedness metric based on Overlap and Decreasing Fill) method (Almeida-Neto & Ulrich, 2011).

2.7 | Statistical modelling of abundance and network metrics in relation to EVI

Linear model analyses were carried out in *R* version 4.2.1. TAI (unadjusted for host intrinsic variables) and EVI means were calculated for each site x year sampling point and were

standardised within sites for both sample sets, using the *scale_by* function in the *standardise* library (Eager, 2017). This effectively converted the TAI and EVI data into anomalies or deviates from the within-site mean. The Egyptian and Polish sampling point anomalies were then concatenated (stacked) into a single dataset and the TAI anomalies were analysed as the response in a linear mixed model with Gaussian errors (LMM) (*lmer* function in the *lme4* package (Bates et al., 2015)), using all of the data, with the EVI anomaly included as a fixed explanatory variable and year (factor) included as a random intercept effect to account for year grouping. A site random term was not included as the variance for this would be zero due to the within-site standardization of the TAI data, which allowed interpretation of model coefficients in terms of standard deviation units for the response and fixed predictors (and reanalysis with unstandardised EVI data and random intercepts for site provided similar interpretations). We repeated the above analysis, in turn replacing TAI with each of the network statistics described above, Weighted modularity Q, Weighted connectance and Weighted nestedness, and additionally including site-standardised sample size as a fixed explanatory variable. We then further considered the addition of (site-standardised) TAI, as an explanatory variable, to the models for the network statistics.

Secondary analyses of abundance, based on mean raw counts, were also carried for phylum-level functional groups, where these were common to both host assemblages and occurred at all sites. These analyses were conducted in LMMs of the form described above that had TAI as the response, using site-standardised data.

Infection abundance in individual taxa has been extensively analysed previously in the present study systems (Behnke et al., 2000, 2001, 2004, 2008a,b, 2019; Bajer at al., 2001, 2005; Siński et al., 2006a,b; Grzybek et al., 2015; Alsarraf et al., 2016) and may be influenced by intrinsic host variables, which is not taken into account in the analysis of TAI above. Using standard linear models (see Supplementary Tables 3-4; *lm* base function), applied to each dataset separately, we confirmed that individual TAI was (positively) influenced by body weight in both datasets (host body weight was the strongest intrinsic predictor of TAI in both datasets, compared to host sex) and that sex was important in the Egyptian dataset. To take the effect of these intrinsic variables into account, we generated random intercepts for site x year sampling points in an LMM (Gaussian errors) (*lmer* function in the *lme4* package) with individual TAI as the response and with fixed terms for body weight (continuous), sex (factor) and site (factor) and random intercepts for site × time point (Supplementary Tables 5-6). Random intercepts were extracted from this model (*ranef* function in *lme4*) and effectively represent TAI site anomalies around the fixed site term, adjusted for host weight and sex by the fixed terms for these. We then re-standardised the random effects to convert the TAI anomalies to standard deviation units and analysed them

as for unadjusted TAI above, with this analysis effectively negating any variation due to weight and sex.

Variation due to different model terms in LMMs was quantified using the *calcVarPart* function in the *variancePartition* library (Hoffman & Schadt, 2016).

2.8 | Trap rate

Trap rates (captures per trap hour), such as those available in this study (Supplementary Table 7) can be used as a relative abundance index (Skalski et al., 2005) for the host, although this is complicated by the possibility of systematic variation in the capture probability for individuals, which cannot be estimated from the available data. Although estimating host abundances was not a primary focus here, we have employed trap rate as a crude proxy for host abundance in some secondary, indicative, analyses. These analyses, relating trap rate to TAI and EVI, were conducted in LMMs of the form described above, using site-standardised data.

3 | RESULTS

3.1 | Site-standardised Enhanced Vegetation Index (EVI) substantially inversely predicted an index of overall infection burden (Total Abundance Index, TAI)

The structure of our dataset is described in detail in the Materials and methods. Briefly, analyses below were based on at least 1108 hosts (depending on missing data values) from two sample sets (Egypt and Poland) comprising 7 sites and a total of 25 site × time point replicates spanning 2000-2012. For hosts within each sample set (*A. dimidiatus* in Egypt and *M. glareolus* in Poland) we constructed a total abundance index (TAI) by summing standardised counts for all infectious agents (see Materials and methods for details). In a combined analysis of the sample sets, where variables were standardised within sites, EVI significantly inversely predicted TAI when analysed in a Linear Mixed Model (LMM) (slope = -0.65±0.16, $P = 5.1 \times 10^{-4}$). This relationship explained more than one third of the variation in TAI (Fig. 1) (44% partitioned variance in the LMM). This was approximately maintained when TAI was adjusted for host sex and weight (slope = -0.54±0.13, $P = 4.1 \times 10^{-4}$; 36% partitioned variance) (see Materials and methods for details). The crude trend was also consistent in the two sample sets (Poland, Pearson r = -0. 70; Egypt, r =-0.73; for site standardised data) (see Fig. 1). A crude proxy for host abundance (trap rate) only weakly predicted TAI (LMM, slope = -0.27±0.13, P = 0.051; 6% partitioned variance) (Fig. 2) and was unrelated to EVI.

To decompose the effect of EVI on overall infection burden, we carried out *post hoc* analyses of mean total counts at site × time sampling points, broken down by phylum-level functional groups, where these were common to both host assemblages and occurred at all sites. This included gastrointestinal nematodes, *Hepatozoon* parasitaemia, *Bartonella* bacteraemia and *Mycoplasma* bacteraemia. There were strong inverse associations with EVI for gastrointestinal nematodes (LMM, slope = -0.56±0.17, $P = 0.0037$) and *Mycoplasma* (slope = -0.77±0.14, $P = 9.4 \times 10^{-6}$) the only two groups present in all time × sites sampling points, and there were non-significant but negative trending associations for *Bartonella* and *Hepatozoon* (see Fig. 2)

3.2 | EVI predicted connectance and modularity in host occupancy networks

We calculated weighted network metrics (connectance, modularity and nestedness) to describe variation in structure in bipartite host occupancy networks for the infectious agent community at each site × year sampling point. Adjusting for host sample size, we found that weighted modularity increased with EVI (LMM, 0.58±0.18, $P = 0.006$; 30% of partitioned variance) and decreased with TAI (-0.78±0.14, $P = 8.4 \times 10^{-6}$; 57% of partitioned variance), with EVI explaining no further variation when added to a model already containing TAI. Weighted connectance, in contrast, decreased with EVI (-0.54±0.18, $P = 0.005$; 25% of partitioned variance) and increased with TAI (0.66±0.16, $P = 0.001$; 45% of partitioned variance), with EVI again explaining no additional variation when added to a model already containing TAI. Thus, weighted connectivity and modularity, which were strongly inversely associated (Pearson r = -0.87 for unstandardised data and -0.78 for site-standardised data), varied as effective proxies of TAI. Weighted nestedness (adjusted for sample size) was unrelated to EVI or the other network statistics, although it decreased with TAI (-0.57±0.21, P = 0.014). None of the network statistics were related to trap rate.

4 | DISCUSSION

We have found that site-standardised remote-sensed vegetation indices are able to inversely predict a substantial amount (more than one third) of the within-habitat variation in an index of overall infection burden over time in two geographically distinct natural rodent host-infectious agent systems. The vegetation indices employed were based on the Enhanced Vegetational Index (EVI) that was standardised (i.e., centred and expressed in standard deviation units) for individual sites. The trend was consistent across the two disparate study areas (Egypt and Poland) and was maintained in the phylum-level pathogen groups universally occurring in all spatiotemporal sampling points. Moreover, we found that site-standardised EVI additionally predicted variation in infectious agent community structure, although only where this was a direct surrogate of overall abundance.

Many previous studies have found that environmental variables, including those measured through remote sensing, may predict infectious agent populations or communities (Froeschke et al., 2010; Krasnov et al., 2010, 2021; Clark et al., 2020; Fecchio et al., 2020; King'ori et al., 2020; Shearer & Ezenwa, 2020; Blersch et al., 2021; Pauling et al., 2021; Carlson et al., 2022; Kosoy & Biggins, 2022; Vinagre-Izquierdo et al., 2022) or zoonotic infection risk (Parmenter et al., 1999; Glass et al., 2000, 2002; Pauling et al., 2021; Redding et al., 2021; Carlson et al., 2022). However, where these have focussed on vegetation predictors, or their correlates, in most cases between-locality variation or within-year variation has been studied, which may have limitations. Thus, between-locality studies may be affected by spatial autocorrelation and confounding due to site-specific variation. Moreover, within-year studies may be affected by temporal autocorrelation, as any circannual (seasonal) variables will be autocorrelated at some time lag. In contrast, long term within-site between-year time series, such as we employ here, allow temporal variations in variables-of-interest to be considered on a relatively level playing field (i.e., on the same background of site characteristics and phase point in the seasonal cycle), increasing the signal to noise ratio and avoiding autocorrelative effects. The present study is thus uniquely powerful in considering two multiannual, decade-spanning time series with regular site replication, allowing a within-site ("site-standardised") approach to be employed.

From a practical point of view, the current study has, using a site-standardised approach, strengthened the proof-of-principle that remotely-sensed vegetation spectra could provide substantial partial forecasting of infection levels, infectious agent community structure and infectious disease risks in natural vertebrate systems. Moreover, the temporally lagged nature of the effects we saw mean that useful forecasts could be made in real-time with lead-in time scales (weeks or months) that allow intervention. Such information could be generated with relatively little difficulty and cost given the high availability of many remote sensing data. It could then, for example, be combined with other sources of information on land use, human populations or animal and pathogen distributions and employed to prioritize local surveillance activity or preparedness according to available resources. Whilst our study focussed on a wide range of haemoparasites (Protozoa) and haemopathogens (Bacteria) and metazoan parasites, we expect that other infectious agents, including viruses, would respond to similar environmental pressures, as they are subject to similar constraints of transmission and host resistance.

Recording many different infections allowed a detailed analysis of community structure. We considered weighted infectious agent community network structure metrics, in addition to abundance, as these might reflect regulatory properties of a community relating to its stability and hence to change in infection risk. We found that some community network

properties were strongly predicted by EVI, but in all cases, in practice, these were also surrogates for total abundance. Thus, in bipartite host co-occupancy networks, network modularity increased and connectance decreased as EVI increased (and as abundance decreased). Although modularity and connectance might be expected to scale passively with network size (Dormann et al., 2009; Dormann & Strauss, 2014), the associations with EVI were maintained when host sample size was adjusted for. Nestedness, which was unrelated to abundance, was also unrelated to EVI. To our knowledge, these are amongst the first observations to relate remotely-sensed primary production to temporal variations in infectious agent community structure.

The direction of the trend in total abundance in relation to EVI that we observed raises important questions. In particular, infectious agent abundance might be predicted to increase with bottom-up productivity and its drivers, such as precipitation and temperature (Felton et al., 2021), due to the facilitated development of larval stages or the amplification of host or vector populations (Arneberg et al., 1998; Mouritsen & Poulin, 2002). A positive influence of primary productivity on infectious agent abundance would also be in line with universal scaling rules based on metabolic theory (Hechinger et al., 2011). In contrast to this expectation we, in fact, observed infectious agent abundance to decrease as EVI increased; and this trend was, in turn, accompanied by changes in network modularity and connectivity. Whilst the present study is focussed on prediction and is not configured to reveal any causal chain between productivity, abundance and community structure, nonetheless, it is useful, from the point of view of circumscribing future hypotheses, to briefly speculate on what the biological drivers for these observed trends might be. One possibility is that the negative association we saw between primary production and overall infection burden is due to a dilution effect, either acting at a community level, through increased biodiversity (Schmidt & Ostfeld, 2001), or at the host population level, through rapid demographic increase in the specific host (Abu-Madi et al., 2003). In the former case, bottom-up trophic cascades might, for example, increase the diversity of organisms similar to the specific hosts of infectious agents, diluting their frequency and reducing successful transmission (Khalil et al., 2016; Loxton et al., 2017; Huang et al., 2017; Stuart et al., 2020; Stewart Merrill & Johnson, 2020; Min et al., 2021; McManus et al., 2021). In the case of a population-level dilution effect, demographic expansion of the specific host populations, again driven by bottom-up trophic cascades, might outstrip the transmission ability of infectious agents. Patterns attributable to the latter process can often be observed in seasonally recruiting rodent populations (Abu-Madi et al., 2003). In either of these scenarios, in addition to dilution effects on abundance, increases in unsuitable or yet-to-be-infected hosts might also increase modularity and decrease connectance. A further possibility is that high primary production might result in

better host nutritional state, elevating immunocompetence (Jackson et al., 2020; Shearer & Ezenwa, 2020). This might limit abundance via host resistance effects and increase modularity, or reduce connectance, through amplified individual immunoheterogeneity (Tinsley et al., 2020). These dilution or immunocompetence scenarios are not mutually exclusive, and other possibilities could also be envisaged, but there is some reason to think that population-level dilution is less likely. As this scenario depends on demographic expansion of the host, it is not supported by our host abundance data, which were not predicted by EVI and only weakly predicted infectious agent abundance. However, we note that the simple trapping rates we recorded do not account for variation in detectability (individual capture probability), which could, putatively, vary systematically with EVI. Thus, more research is required to distinguish between the possibilities set out above, or other possibilities, and to understand the processes determining the links between EVI and infectious agent abundance and community structure observed here.

Our results have important implications for the effect of global environmental change on infectious disease risk in natural vertebrate wildlife reservoirs, given the recent broad worldwide greening trend (Nemani et al., 2003; Mao et al., 2016; Zhu et al., 2016; Buitenwerf et al., 2018; Winkler et al., 2019). As disease transmission risk would be expected to increase with pathogen abundance, all other things being equal, and as we observed abundance to decrease with EVI (greening) here, it seems likely that otherwise stable habitats with increasing productivity would be subject to decreasing infectious disease risk. More tentatively, the changes that we observed in community structure as EVI increased might also affect disease risk through altering community stability. Notably, this possibility depends on the existence of interspecific interactions that might act as stabilising or destabilising feedbacks, and for which there is some evidence in wild vertebrate systems (Lello et al., 2004; Behnke et al., 2005, 2009; Jackson et al., 2006; Behnke, 2008, 2009; Ferrari et al., 2009; Telfer et al., 2010; Knowles et al., 2013; Pedersen & Antonovics, 2013; Lewis et al., 2023). In the present dataset we observed modularity to increase and connectance to decrease with increasing EVI, with both connectance and modularity effectively being proxies of abundance. Increasing modularity and decreasing connectance would be linked to increasing stability in classical theoretical studies of random networks (May, 1972). On the other hand, this may not apply in the non-random set of network structures that occur in real ecological situations (Pimm, 1979; Solow et al., 1999; Teng & McCann, 2004; Stouffer & Bascompte, 2011), which may be subject to effects in the opposite direction, i.e., destabilizing effects in respect of the trends that we observed here. Thus, whilst we are currently unable predict the nature of effects on stability resulting from the EVI-linked changes in modularity and connectance seen here, there is evidence from the

wider literature on ecological networks that these community properties could affect stability (Grilli et al., 2016; Landi et al., 2018; Baumgartner, 2020, Bascompte & Scheffer, 2023). Clearly, more research is required on the stability properties of the community structures of infectious agents.

It is possible that including more remotely-sensed variables affecting infectious agent transmission and establishment might ultimately increase the encouraging predictiveness we have observed here. In our current study we *a priori* focussed specifically on EVI due to its embodiment of primary productivity, which we expected (as set out in the Introduction) to drive infection levels through effects on host availability and host immunocompetence. However, we note that EVI would also be expected to correlate with other environmental variables, such as temperature or precipitation (Felton et al., 2021), that might have separate, direct effects on infectious agent dynamics (Arneberg et al., 1998; Mouritsen & Poulin, 2002). For example, temperature change may alter the rate of development or the survival of infective stages, whilst precipitation may also alter the dynamics of transmission in free-living stages. Whilst all of these processes might not always drive infection burden in the same direction, nonetheless, our present result suggests that, overall, there may be a consistent pattern. Thus, EVI, with its links to primary production, precipitation and temperature seems likely to provide a valuable "all-in-one" predictor, but more work, with new datasets, is necessary to assess additional predictors and also to assess the optimal time intervals and time lags at which EVI is most predictive.

In conclusion, we have shown proof-of-principle that remotely-sensed data, reflecting primary productivity, can predict fluctuations in the burden and community structure of infections in wild vertebrates in near-real-time, when standardised within localities. The sequels of greening that we observed in infectious agent communities seem most likely to limit the spread of infection and the chance of transboundary emergence. Thus, greening is associated with overall decreases in the burden of infection that would be expected to reduce the probability of transmission. Moreover, greening is also associated with increased modularity and diminished connectance in the infectious agent community. These tendencies may affect community stability, which, in turn, might determine the propensity for novel community dynamics leading to new infection risks. Given the recent clear overall worldwide greening trend (Nemani et al., 2003; Mao et al., 2016; Zhu et al., 2016; Buitenwerf et al., 2018; Winkler et al., 2019), albeit with some evidence this may be slowing down, or patchy on some geographical scales (Winkler et al., 2021)), our results suggest that, at least in stable habitats (i.e., those not disrupted by new human encroachment or excessive climate driven change), infection risks may have been diminishing, all other things being equal. Recent studies of global land use change have predicted drastic future mass

extinctions of parasites (up to 30% of parasitic worm species by 2070) due to loss of habitat (Carlson et al., 2017), which might have a suppressive influence on global infection risks. Moreover, our results suggest this could be compounded, assuming continued greening, in surviving intact habitats, by within-habitat reduction in the overall abundance of infectious agents. On the other hand, in the case of greening trends decelerating, our results may give cause for concern. Whilst zoonotic emergence has been observed to increase overall in recent decades, which has been attributed mostly to anthropogenic disturbance of natural habitats (Eby et al., 2023), this trend may have been restrained, if our present results are correct, by declining infection risks from relatively undisturbed ecoystems (for example, potentially reducing the set of pathogens available for transboundary emergence in habitats prior to disturbance). Thus, if greening were to slow or reverse in the future, our findings suggest the rate of zoonotic emergence would accelerate (for example, increasing the set of pathogens available for transboundary emergence when habitats are disturbed). In practical terms, our results provide optimism that routinely collected remote-sensing data could provide useful low-cost forecasting of changing within-habitat infection risk in natural animal populations. We suggest that more research is warranted to explore this possibility, including to elucidate the intervening causal chain and dynamics that link primary productivity to fluctuations in natural communities of infectious agents.

ACKNOWLEDGEMENTS

The fieldwork in both Poland and Egypt was supported by travel grants from the Universities of Nottingham and Warsaw, the Royal Society (JMB) and the British Ecological Society (JMB). We also received financial support from the British Council in Cairo in 2000 (a LINK grant between Nottingham and Suez Canal University [FSG]). The 2008 expedition led by AB was supported financially by KBN-BC Young Scientist Program no. WAW/342/06. The 2012 expedition by Polish staff was funded by the National Science Centre (NCN), Poland, grant OPUS 2011/03/B/NZ6/02090 (AB) and by the Ministry of Science and Higher Education through the Faculty of Biology, University of Warsaw's intramural grant DSM number 140000/501/86-110101. We are grateful to NASA's Land Processes Distributed Active Archive Center (LP DAAC) for access to remotely-sensed data and to the University of Salford for supporting analytical work. In Poland, we thank Mgrs Grzegorz Górecki and Anna Zaborowska, the wardens of the field station at Urwitałt, for the use of the facilities, and we acknowledge the support of the forestry departments responsible for the woodland sites utilized in our study (Nadleśnictwa Giżycko, Mikołajki and Orzysz). In Egypt, we thank Professor Samy Zalat and all the staff of the Environment Research Centre of Suez Canal

University as well as our Bedouin hosts led by Faraj Mahmoud from Fox Camp at St. Katherine. Their support and warm hospitality during our stay in St. Katherine and in the camps in the more distant study sites (Hussein Saleh, Jemil Attiya Hussein & Nasr Mansur) was much appreciated. We thank the Egyptian Environmental Affairs Agency and the Protectorate managers Dr John Grainger, Mohammed Shaker and Mohamed Qotb for permission to work in St. Katherine Protectorate, and the staff at the Rangers office for providing vehicles and drivers to enable access to some of the remote locations and for their company and support on each of the expeditions. Finally, but not least, we thank Professors E. Sinski and P. Harris and all the undergraduate student helpers from both The University of Nottingham and The University of Warsaw who helped with fieldwork during the eight expeditions to our study sites and with subsequent laboratory work at both the universities.

AUTHOR CONTRIBUTIONS

Study design: JMB, AB and FSG. Fieldwork: JMB, AB, JBB, MG, MA and many student helpers. Laboratory analysis: JMB, AB, JBB, MG, MA and many student helpers. Data analysis: JAJ. Writing: JAJ and JMB. All authors read and agreed the published version of this manuscript.

DATA ACCESSIBILITY

The data that support the findings of this study are openly available in Zenodo at http://doi.org/10.5281/zenodo.8182747, reference number 8182747.

REFERENCES

Abu-Madi M. A., Behnke J. M., Lewis J. W., Gilbert F. S. Seasonal and site specific variation in the component community structure of intestinal helminths in *Apodemus sylvaticus* from three contrasting habitats in south-east England. *J. Helminthol.* **74**, 7-15 (2000).

Almeida-Neto M., Ulrich W. A straightforward computational approach for measuring nestedness using quantitative matrices. *Environ. Model. & Softw.* **26**, 173-178 (2011).

Alsarraf M.*, et al.* Long-term spatiotemporal stability and dynamic changes in the haemoparasite community of spiny mice (*Acomys dimidiatus*) in four montane wadis in the St. Katherine Protectorate, Sinai, Egypt. *Parasit. Vectors* **9**, 195 (2016).

AppEEARS Team. Application for extracting and exploring analysis ready samples (AppEEARS). NASA EOSDIS Land Processes Distributed Active Archive Center (LP DAAC), USGS/Earth Resources Observation and Science (EROS) Center, Sioux Falls, South Dakota, USA (2023).

Arneberg P., Skorping A., Grenfell B., Read A. F. Host densities as determinants of abundance in parasite communities. *Proc. Biol. Sci.* **265**, 1283-1289 (1998).

Bajer A., Behnke J. M., Pawełczyk A., Kuliś K., Sereda M. J., Siński E. Medium-term temporal stability of the helminth component community structure in bank voles (*Clethrionomys glareolus*) from the Mazury Lake District region of Poland. *Parasitology* **130**, 213-228 (2005).

Bajer A., Pawelczyk A., Behnke J. M., Gilbert F. S., Sinski E. Factors affecting the component community structure of haemoparasites in bank voles (*Clethrionomys glareolus*) from the Mazury Lake District region of Poland. *Parasitology* **122**, 43-54 (2001).

Bascompte J., Scheffer M. The resilience of plant–pollinator networks. *Ann. Rev. Entom.* **68**, 363-380 (2023).

Bates D., Mächler M., Bolker B., Walker S. Fitting Linear Mixed-Effects Models Using lme4. *J. Stat. Softw.* **67**, 1 - 48 (2015).

Baumgartner M. T. Connectance and nestedness as stabilizing factors in response to pulse disturbances in adaptive antagonistic networks. *J. Theor. Biol.* **486**, 110073 (2020).

Becker D. J., Eby P., Madden W., Peel A. J., Plowright R. K. Ecological conditions predict the intensity of Hendra virus excretion over space and time from bat reservoir hosts. *Ecol. Lett.* **26**, 23-36 (2023).

Behnke J. M. Structure in parasite component communities in wild rodents: predictability, stability, associations and interactions .... or pure randomness? *Parasitology* **135**, 751-766 (2008).

Behnke J. M. Detecting interactions between parasites in cross-sectional studies of wild rodent populations. *Wiad. Parazytol.* **55**, 305-314 (2009).

Behnke J. M.*, et al.* Long-term spatiotemporal stability and dynamic changes in helminth infracommunities of spiny mice (*Acomys dimidiatus*) in St. Katherine's Protectorate, Sinai, Egypt. *Parasitology* **146**, 50-73 (2019).

Behnke J. M.*, et al.* Temporal and between-site variation in helminth communities of bank voles (*Myodes glareolus*) from N.E. Poland. 1. Regional fauna and component community levels. *Parasitology* **135**, 985-997 (2008a).

Behnke J. M.*, et al.* Temporal and between-site variation in helminth communities of bank voles (*Myodes glareolus*) from N.E. Poland. 2. The infracommunity level. *Parasitology* **135**, 999-1018 (2008b).

Behnke J. M.*, et al.* Variation in the helminth community structure in bank voles (*Clethrionomys glareolus*) from three comparable localities in the Mazury Lake District region of Poland. *Parasitology* **123**, 401-414 (2001).

Behnke J. M.*, et al.* Intestinal helminths of spiny mice (*Acomys cahirinus dimidiatus*) from St Katherine's Protectorate in the Sinai, Egypt. *J. Helminthol.* **74**, 31-43 (2000).

Behnke J. M.*, et al.* Helminth species richness in wild wood mice, *Apodemus sylvaticus*, is enhanced by the presence of the intestinal nematode *Heligmosomoides polygyrus*. *Parasitology* **136**, 793-804 (2009).

Behnke J. M., Gilbert F. S., Abu-Madi M. A., Lewis J. W. Do the helminth parasites of wood mice interact? *J. Anim. Ecol.* **74**, 982-993 (2005).

Behnke J. M.*, et al.* Variation in the helminth community structure in spiny mice (*Acomys dimidiatus*) from four montane wadis in the St Katherine region of the Sinai Peninsula in Egypt. *Parasitology* **129**, 379-398 (2004).

Bernstein A. S*., et al.* The costs and benefits of primary prevention of zoonotic pandemics. *Sci. Adv.* **8**, eabl4183 (2022).

Bersier L.-F., Banašek-Richter C., Cattin M.-F. Quantitative descriptors of food web matrices. *Ecology* **83**, 2394-2407 (2002).

Blersch R., Bonnell T. R., Barrett L., Henzi S. P. Seasonal effects in gastrointestinal parasite prevalence, richness and intensity in vervet monkeys living in a semi-arid environment. *J. Zool.* **314**, 163-173 (2021).

Bordes F., Morand S. Parasite diversity: an overlooked metric of parasite pressures? *Oikos* **118**, 801-806 (2009).

Buitenwerf R., Sandel B., Normand S., Mimet A., Svenning J.-C. Land surface greening suggests vigorous woody regrowth throughout European semi-natural vegetation. *Glob. Chang. Biol.* **24**, 5789-5801 (2018).

Carlson C. J., Bevins S. N., Schmid B. V. Plague risk in the western United States over seven decades of environmental change. *Glob. Chang. Biol.* **28**, 753-769 (2022).

Carlson C. J*., et al.* Parasite biodiversity faces extinction and redistribution in a changing climate. *Sci. Adv.* **3**, e1602422 (2017).

Chávez R. O*., et al.* GIMMS NDVI time series reveal the extent, duration, and intensity of "blooming desert" events in the hyper-arid Atacama Desert, Northern Chile. *Int. J. Appl. Earth Obs. Geoinf.* **76**, 193-203 (2019).

Clark N. J., Drovetski S. V., Voelker G. Robust geographical determinants of infection prevalence and a contrasting latitudinal diversity gradient for haemosporidian parasites in Western Palearctic birds. *Mol. Ecol.* **29**, 3131-3143 (2020).

Dall'Olmo G., Karnieli A. Monitoring phenological cycles of desert ecosystems using NDVI and LST data derived from NOAA-AVHRR imagery. *Int.l J. Remote Sens.* **23**, 4055-4071 (2002).

Delmas E*., et al.* Analysing ecological networks of species interactions. *Biol. Rev.* **94**, 16-36 (2019).

de Vos M. G. J., Zagorski M., McNally A., Bollenbach T. Interaction networks, ecological stability, and collective antibiotic tolerance in polymicrobial infections. *Proc. Natl Acad. Sci. USA* **114**, 10666-10671 (2017).

Didan, K., Huete, A., MODIS Adaptive Processing System (MODAPS) Science Investigator-led Processing Systems (SIPS). MOD13Q1 MODIS/Terra Vegetation Indices 16-Day L3 Global 250m SIN Grid. NASA Land Processes Distributed Active Archive Center (LP DAAC) (2015). http://doi.org/10.5067/MODIS/MOD13Q1.006

Didan K., Munoz A. B., Solano R., Huete A. MODIS vegetation index user's guide (MOD13 series). *University of Arizona: Vegetation Index and Phenology Lab*, 35 (2015).

Dobson A. P*., et al.* Ecology and economics for pandemic prevention. *Science* **369**, 379-381 (2020).

Dormann C. F., Fründ J., Blüthgen N., Gruber B. Indices, graphs and null models: analyzing bipartite ecological networks. *Open Ecol. J.* **2**, 7-24. (2009).

Dormann C. F., Gruber B., Fründ J. Introducing the bipartite Package: Analysing Ecological Networks. *The R Journal* **8**, 8-11 (2008).

Dormann C. F., Strauss R. A method for detecting modules in quantitative bipartite networks. *Methods Ecol. Evol.* **5**, 90-98 (2014).

Eager C. Standardise: tools for standardizing variables for regression in R. R package version 0.2.1.(2017).

Eby P.*, et al.* Pathogen spillover driven by rapid changes in bat ecology. *Nature* **613**, 340-344 (2023).

Fecchio A.*, et al.* An inverse latitudinal gradient in infection probability and phylogenetic diversity for *Leucocytozoon* blood parasites in New World birds. *J. Anim. Ecol.* **89**, 423-435 (2020).

Felton A. J., Knapp A. K., Smith M. D. Precipitation–productivity relationships and the duration of precipitation anomalies: An underappreciated dimension of climate change. *Glob. Chang. Biol.* **27**, 1127-1140 (2021).

Fernández N., Román J., Delibes M. Variability in primary productivity determines metapopulation dynamics. *Proc. Biol. Sci.* **283**, 20152998 (2016).

Ferrari N., Cattadori I. M., Rizzoli A., Hudson P. J. *Heligmosomoides polygyrus* reduces infestation of *Ixodes ricinus* in free-living yellow-necked mice, *Apodemus flavicollis*. *Parasitology* **136**, 305-316 (2009).

Froeschke G., Harf R., Sommer S., Matthee S. Effects of precipitation on parasite burden along a natural climatic gradient in southern Africa – implications for possible shifts in infestation patterns due to global changes. *Oikos* **119**, 1029-1039 (2010).

Glass G. E.*, et al.* Satellite imagery characterizes local animal reservoir populations of Sin Nombre virus in the southwestern United States. *Proc. Natl Acad. Sci. USA* **99**, 16817-16822 (2002).

Glass G. E.*, et al.* Using remotely sensed data to identify areas at risk for hantavirus pulmonary syndrome. *Emerg. Infect. Dis.* **6**, 238-247 (2000).

Gotelli N. J., Shimadzu H., Dornelas M., McGill B., Moyes F., Magurran A. E. Community-level regulation of temporal trends in biodiversity. *Sci. Adv.* **3**, e1700315 (2017).

Grilli J., Rogers T., Allesina S. Modularity and stability in ecological communities. *Nat. Comm.* **7**, 12031 (2016).

Grzybek M.*, et al.* Long-term spatiotemporal stability and dynamic changes in helminth infracommunities of bank voles (*Myodes glareolus*) in NE Poland. *Parasitology* **142**, 1722-1743 (2015).

Han B. A., Kramer A. M., Drake J. M. Global Patterns of Zoonotic Disease in Mammals. *Trends Parasitol.* **32**, 565-577 (2016).

Häsler B., Gilbert W., Jones B. A., Pfeiffer D. U., Rushton J., Otte M. J. The economic value of One Health in relation to the mitigation of zoonotic disease risks. In: *One Health: The Human-Animal-Environment Interfaces in Emerging Infectious Diseases: The Concept and Examples of a One Health Approach* (eds Mackenzie JS, Jeggo M, Daszak P, Richt JA). Springer Berlin Heidelberg (2013).

Hechinger R. F., Lafferty K. D., Dobson A. P., Brown J. H., Kuris A. M. A common scaling rule for abundance, energetics, and production of parasitic and free-living species. *Science* **333**, 445-448 (2011).

Hoffman, G. E., Schadt, E. E. variancePartition: interpreting drivers of variation in complex gene expression studies. *BMC Bioinformatics* **17**, 483 (2016).

Huang Z. Y., Yu Y., Van Langevelde F., De Boer W. F. Does the dilution effect generally occur in animal diseases? *Parasitology* **144**, 823-826 (2017).

Huete A. R. Vegetation indices, remote sensing and forest monitoring. *Geogr. Compass* **6**, 513-532 (2012).

Huete A., Didan K., Miura T., Rodriguez E. P., Gao X., Ferreira L. G. Overview of the radiometric and biophysical performance of the MODIS vegetation indices. *Remote Sens. Environ.* **83**, 195-213 (2002).

Jackson J. A.*, et al.* Partitioning the environmental drivers of immunocompetence. *Sci. Total Environ.* **747**, 141152 (2020).

Jackson J. A., Pleass R. J., Cable J., Bradley J. E., Tinsley R. C. Heterogeneous interspecific interactions in a host-parasite system. *Int. J. Parasitol.* **36**, 1341-1349 (2006).

Khalil H., Ecke F., Evander M., Magnusson M., Hörnfeldt B. Declining ecosystem health and the dilution effect. *Sci. Rep.* **6**, 1-11 (2016).

King'ori E., Obanda V., Chiyo P. I., Soriguer R. C., Morrondo P., Angelone S. Patterns of helminth infection in Kenyan elephant populations. *Parasit. Vects* **13**, 145 (2020).

Knowles S. C., Fenton A., Petchey O. L., Jones T. R., Barber R., Pedersen A. B. Stability of within-host-parasite communities in a wild mammal system. *Proc. Biol. Sci.* **280**, 20130598 (2013).

Kosoy M., Biggins D. Plague and Trace Metals in Natural Systems. *Int. J. Environ. Res. Public Health* **19**, (2022).

Krasnov B. R.*, et al.* Similarity in ectoparasite faunas of Palaearctic rodents as a function of host phylogenetic, geographic or environmental distances: which matters the most? *Int. J. Parasitol.* **40**, 807-817 (2010).

Krasnov B. R., Vinarski M. V., Korallo-Vinarskaya N. P., Shenbrot G. I., Khokhlova I. S. Species associations in arthropod ectoparasite infracommunities are spatially and temporally variable and affected by environmental factors. *Ecol. Entomol.* **46**, 1254-1265 (2021).

Krügel M., Król N., Kempf V. A. J., Pfeffer M., Obiegala A. Emerging rodent-associated Bartonella: a threat for human health? *Parasit. Vectors* **15**, 113 (2022).

Landi P., Minoarivelo H. O., Brännström Å., Hui C., Dieckmann U. Complexity and stability of ecological networks: a review of the theory. *Popul. Ecol.* **60**, 319-345 (2018).

Lello J., Boag B., Fenton A., Stevenson I. R., Hudson P. J. Competition and mutualism among the gut helminths of a mammalian host. *Nature* **428**, 840-844 (2004).

Lewis J. W., Morley N. J., Behnke J. M. Helminth parasites of the wood mouse *Apodemus sylvaticus* in Southern England: levels of infection, species richness and interactions between species. *J. Helminthol.* **97**, e18 (2023).

Loxton K. C., Lawton C., Stafford P., Holland C. V. Parasite dynamics in an invaded ecosystem: helminth communities of native wood mice are impacted by the invasive bank vole. *Parasitology* **144**, 1476-1489 (2017).

Luis A. D.*, et al.* A comparison of bats and rodents as reservoirs of zoonotic viruses: are bats special? *Proc. Biol. Sci.* **280**, 20122753 (2013).

May R. M. Will a large complex system be stable? *Nature* **238**, 413-414 (1972).

Mao J.*, et al.* Human-induced greening of the northern extratropical land surface. *Nat. Clim. Chang.* **6**, 959-963 (2016).

McManus A., Holland C. V., Henttonen H., Stuart P. The Invasive Bank Vole (*Myodes glareolus*): A model system for studying parasites and ecoimmunology during a biological invasion. *Animals* **11**, (2021).

Min K.-D., Hwang J., Schneider M. C., So Y., Lee J.-Y., Cho S.-I. An exploration of the protective effect of rodent species richness on the geographical expansion of Lassa fever in West Africa. *PLoS Negl. Trop. Dis.* **15**, e0009108-e0009108 (2021).

Moat J.*, et al.* Seeing through the clouds – Mapping desert fog oasis ecosystems using 20 years of MODIS imagery over Peru and Chile. *Int. J. Appl. Earth Obs. Geoinf.* **103**, 102468 (2021).

Mouritsen K. N., Poulin R. Parasitism, climate oscillations and the structure of natural communities. *Oikos* **97**, 462-468 (2002).

Nemani R. R.*, et al.* Climate-driven increases in global terrestrial net primary production from 1982 to 1999. *Science* **300**, 1560-1563 (2003).

Norfolk O., Abdel-Dayem M., Gilbert F. Rainwater harvesting and arthropod biodiversity within an arid agro-ecosystem. *Agric. Ecosyst. Environ.* **162**, 8-14 (2012).

Norfolk O., Eichhorn M. P., Gilbert F. Traditional agricultural gardens conserve wild plants and functional richness in arid South Sinai. *Basic and Appl. Ecol.* **14**, 659-669 (2013).

Norfolk O., Power A., Eichhorn M. P., Gilbert F. Migratory bird species benefit from traditional agricultural gardens in arid South Sinai. *J. Arid Environ.* **114**, 110-115 (2015).

Olson D. M.*, et al.* Terrestrial ecoregions of the world: a new map of life on Earth: a new global map of terrestrial ecoregions provides an innovative tool for conserving biodiversity. *BioScience* **51**, 933-938 (2001).

Parmenter R. R., Yadav E. P., Parmenter C. A., Ettestad P., Gage K. L. Incidence of plague associated with increased winter-spring precipitation in New Mexico. *The Am. J. Trop. Med. Hyg.* **61**, 814-821 (1999).

Pauling C. D., Finke D. L., Anderson D. M. Interrelationship of soil moisture and temperature to sylvatic plague cycle among prairie dogs in the Western United States. *Integr. Zool.* **16**, 852-867 (2021).

Pedersen A. B., Antonovics J. Anthelmintic treatment alters the parasite community in a wild mouse host. *Biol. Lett.* **9**, 20130205 (2013).

Pimm S. L. The structure of food webs. *Theor. Popul. Biol.* **16**, 144-158 (1979).

Plowright R. K.*, et al.* Pathways to zoonotic spillover. *Nat. Rev. Microbiol.* **15**, 502-510 (2017).

Poulin R. Network analysis shining light on parasite ecology and diversity. *Trends Parasitol.* **26**, 492-498 (2010).

Poulin R., McDougall C. Fish–parasite interaction networks reveal latitudinal and taxonomic trends in the structure of host–parasite associations. *Parasitology* **149**, 1815-1821 (2022).

R core Team. R: A language and environment for statistical computing. R Foundation for Statistical Computing (2022).

Redding D. W.*, et al.* Geographical drivers and climate-linked dynamics of Lassa fever in Nigeria. *Nat. Comm.* **12**, 5759 (2021).

Rubenina I.*, et al.* Environmental, anthropogenic, and spatial factors affecting species composition and species associations in helminth communities of water frogs (Pelophylax esculentus complex) in Latvia. *Parasitol. Res.* **120**, 3461-3474 (2021).

Saltz D., Schmidt H., Rowen M., Karnieli A., Ward D., Schmidt I. Assessing grazing impacts by remote sensing in hyper-arid environments. *Rangeland Ecology & Management* **52**, 500-507 (1999).

Santini L.*, et al.* Global drivers of population density in terrestrial vertebrates. *Glob. Ecol. Biogeogr.* **27**, 968-979 (2018).

Schmidt K. A., Ostfeld R. S. Biodiversity and the dilution effect in disease ecology. *Ecology* **82**, 609-619 (2001).

Shearer C. L., Ezenwa V. O. Rainfall as a driver of seasonality in parasitism. *Int. J. Parasitol. Parasites Wildl.* **12**, 8-12 (2020).

Shi H.*, et al.* Assessing the ability of MODIS EVI to estimate terrestrial ecosystem gross primary production of multiple land cover types. *Ecol. Indic.* **72**, 153-164 (2017).

Sims D. A.*, et al.* On the use of MODIS EVI to assess gross primary productivity of North American ecosystems. *J. Geophys. Res. Biogeosci.* **111**, G04015 (2006).

Siński E., Bajer A., Welc R., Pawełczyk A., Ogrzewalska M., Behnke J. M. Babesia microti: prevalence in wild rodents and *Ixodes ricinus* ticks from the Mazury Lakes District of North-Eastern Poland. *Int. J. Med. Microbiol.* **296 Suppl 40**, 137-143 (2006a).

Siński E., Pawełczyk A., Bajer A., Behnke J. Abundance of wild rodents, ticks and environmental risk of Lyme borreliosis: a longitudinal study in an area of Mazury Lakes district of Poland. *Ann. Agric. Environ. Med.* **13**, 295-300 (2006b).

Skalski J. R., Ryding K. E., Millspaugh J., Millspaugh J. *Wildlife Demography : Analysis of Sex, Age, and Count Data*. Elsevier Science & Technology (2005).

Solow A. R., Costello C., Beet A. On an early result on stability and complexity. *Am. Nat.* **154**, 587-588 (1999).

Stenseth N. C.*, et al.* No evidence for persistent natural plague reservoirs in historical and modern Europe. *Proc. Natl Acad. Sci. USA* **119**, e2209816119 (2022).

Stewart Merrill T. E., Johnson P. T. J. Towards a mechanistic understanding of competence: a missing link in diversity–disease research. *Parasitology* **147**, 1159-1170 (2020).

Stouffer D. B., Bascompte J. Compartmentalization increases food-web persistence. *Proc. Natl Acad. Sci. USA* **108**, 3648-3652 (2011).

Stuart P., Paredis L., Henttonen H., Lawton C., Ochoa Torres C. A., Holland C. V. The hidden faces of a biological invasion: parasite dynamics of invaders and natives. *Int. J. Parasitol.* **50**, 111-123 (2020).

Telfer S.*, et al.* Species interactions in a parasite community drive infection risk in a wildlife population. *Science* **330**, 243-246 (2010).

Teng J., McCann K. S. Dynamics of compartmented and reticulate food webs in relation to energetic flows. *Am. Nat.* **164**, 85-100 (2004).

Tinsley R. C., Rose Vineer H., Grainger-Wood R., Morgan E. R. Heterogeneity in helminth infections: factors influencing aggregation in a simple host-parasite system. *Parasitology* **147**, 65-77 (2020).

Vinagre-Izquierdo C.*, et al.* The drivers of avian-haemosporidian prevalence in tropical lowland forests of New Guinea in three dimensions. *Ecol. Evol.* **12**, e8497 (2022).

Wallace C. S. A., Thomas K. A. An annual plant growth proxy in the Mojave Desert using MODIS-EVI Data. *Sensors (Basel)* **8**, 7792-7808 (2008).

Wang Y., Roderick M. L., Shen Y., Sun F. Attribution of satellite-observed vegetation trends in a hyper-arid region of the Heihe River basin, Western China. *Hydrol. Earth Syst. Sci.* **18**, 3499-3509 (2014).

Wille M., Geoghegan J. L., Holmes E. C. How accurately can we assess zoonotic risk? *PLoS Biol.* **19**, e3001135 (2021).

Winkler A. J., Myneni R. B., Alexandrov G. A., Brovkin V. Earth system models underestimate carbon fixation by plants in the high latitudes. *Nat. Comm.* **10**, 885 (2019).

Winkler A. J.*, et al.* Slowdown of the greening trend in natural vegetation with further rise in atmospheric CO2. *Biogeosciences* **18**, 4985-5010 (2021).

WMO. *The Global Climate 2001-2010: A decade of climate extremes: summary report*. World Meteorological Organization (2013).

Xu L., Schmid B. V., Liu J., Si X., Stenseth N. C., Zhang Z. The trophic responses of two different rodent–vector–plague systems to climate change. *Proc. Biol. Sci.* **282**, 20141846 (2015).

Young K. M.*, et al.* Zoonotic Babesia: A scoping review of the global evidence. *PLoS One* **14**, e0226781-e0226781 (2019).

Zhou Y., Zhang L., Xiao J., Chen S., Kato T., Zhou G. A Comparison of satellite-derived vegetation indices for approximating gross primary productivity of grasslands. *Rangel. Ecol. Manag.* **67**, 9-18 (2014).

Zhu Z.*, et al.* Greening of the Earth and its drivers. *Nat. Clim. Chang.* **6**, 791-795 (2016).

Figure 1. Association between Total Abundance Index (TAI), reflecting overall infection burden, and Enhanced Vegetation Index (EVI), reflecting primary productivity in the quarter before sampling. Based on a linear mixed model (LMM) run with site-standardised data. Shown are the predicted effect (solid line) with 95% confidence limits (dashed lines) and partial residuals for site × year sampling points.

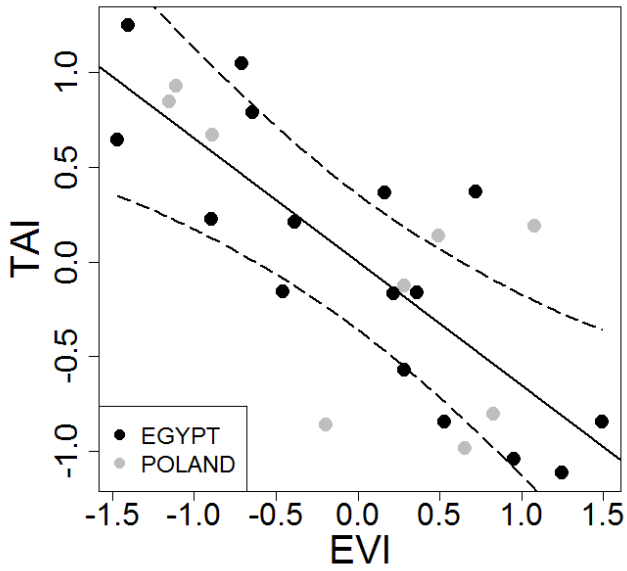

Figure 2. Association between abundance (mean raw counts) of phylum-level groups and Enhanced Vegetation Index (EVI), reflecting primary productivity in the quarter before sampling. Based on linear mixed models (LMMs) run with site-standardised data. Shown are the predicted effects (solid lines) with 95% confidence limits (dashed lines) and partial residuals for site × year sampling points (black points, Egypt; grey points, Poland). GI: gastrointestinal.

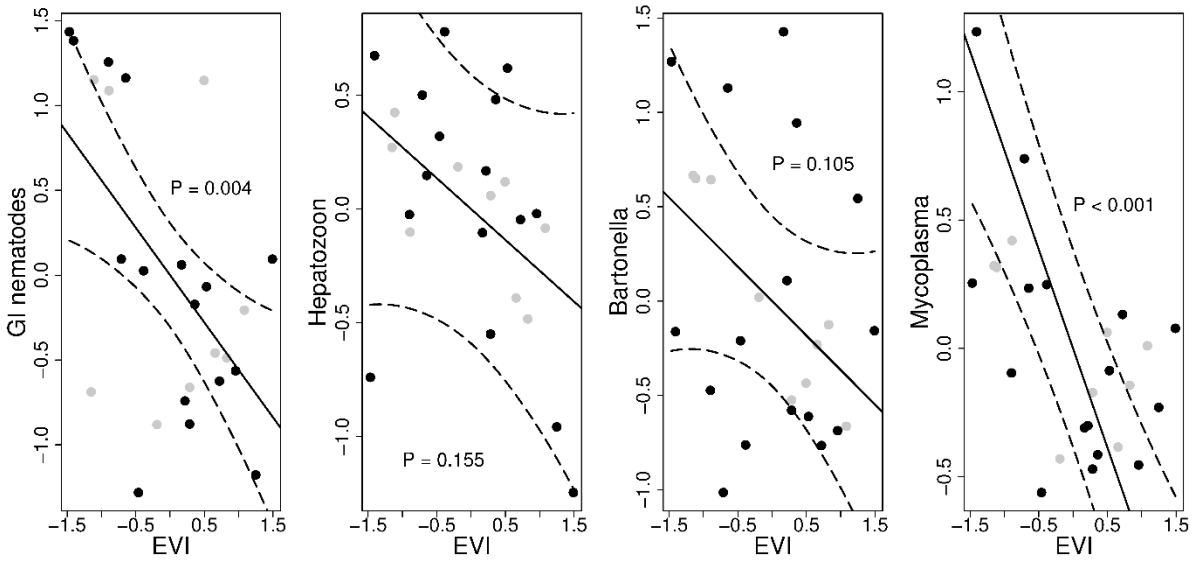

Figure 3. Variation in network statistics with the Enhanced Vegetation Index (EVI), reflecting primary productivity in the quarter before sampling, and with Total Abundance Index (TAI), reflecting overall infection burden. The four left-hand panels are based on linear mixed models (LMMs) run with site-standardised data; shown are the predicted effects (solid lines) with 95% confidence limits (dashed lines) and partial residuals for site × year sampling points (black points, Egypt; grey points, Poland). The right-hand panel shows the crude association between site-standardised weighted connectance and weighted modularity, with a least squares regression line shown for reference (black points, Egypt; grey points, Poland).